Asian Journal of Chemistry; Vol. 31, No. 8 (2019), 1791-1797

ASIAN JOURNAL OF CHEMISTRY

https://doi.org/10.14233/ajchem.2019.22043

Characterization of Natural Rubber/Polyethylene Oxide (NR/PEO) Block Copolymer-Metal Ion Chelates

M.S. MRUDULA and M.R. GOPINATHAN NAIR*

School of Chemical Sciences, Mahatma Gandhi University, Kottayam-686560, India

*Corresponding author: E-mail: mrgnairscs@gmail.com

Received: 1 March 2019; *Accepted*: 3 April 2019; *Published online*: 28 June 2019; AJC-19453

Two shot solution polymerized natural rubber/polyethylene oxide (NR/PEO) block copolymers are used as chelating exchanger for the metal ions Mn(II) and Fe(II). The polymer - metal ion chelates are prepared *via* solution batch adsorption method and are subjected to various characterisation techniques. Adsorption studies shows 96 and 63 % complexation for Mn(II) and Fe(III) ions, respectively. The 7_2 helical conformation of PEO and metal-etheric oxygen coordination are confirmed by FT-IR spectroscopy. The XRD results revealed the complete miscibility of metal ions and semi-crystalline nature of samples. The EDX analysis confirmed the presence of metal ions in the polymer chelates. Surface morphology is also studied using SEM and TEM techniques.

Keywords: Natural rubber, Polyethylene oxide, Block copolymer, Polymer chelate, Adsorption.

INTRODUCTION

Polymer-metal complex become an important area in material chemistry due to their interesting properties and applications. In metal complexation the inorganic metal ions are coordinated to the ligands either by ionic bond, coordination bond or by ion-dipole interactions. The technique of polymer-metal complexation can be applied in wastewater treatment to remove toxic metal ions, separation of metal ions, to improve mechanical and thermal properties of polymers and in polymer-metal catalyst [1-6].

Block copolymers are excellent material for the metal ion complexation from aqueous medium. Block copolymers prepared from monomers which differ in physical and chemical properties shows superior properties than blends and random copolymers. Wide varieties of block copolymers were prepared and can be used as thermoplastic elastomers, drug carriers, membranes for metal ion removal, surfactants, *etc*. [7]. Ambhiphilic block copolymers were become most interesting class of block copolymers and many researches are still ongoing. Many researchers [8-10] used polyethylene oxide (PEO) as hydrophilic component and is copolymerized with an elastomer to obtain good mechanical properties. These PEO based polymers can find application in the field of removal, recovery, complexation of metal ions from aqueous medium, solid polymer electrolytes, dielectrics, *etc*. The metal ion binding of PEO is a well-known process which mimics the cation complexation of crown ethers and widely studied the interaction between PEO and metal ions [11-15].

The wonderful semicrystalline polymer (polyethylene oxide, PEO), was extensively studied and prepared many of its metal ion complexes from various applications which are characterised by means of different techniques [16-22]. The better knowledge on the structural, morphological and thermal properties helps to prepare application defined polymer-metal complexes. The poor mechanical property and solubility of PEO are the major drawbacks of PEO-metal ion complexes for various applications. To overcome low mechanical stability and to improve user defined properties many researchers copolymerized PEO with other polymers [23-25]. Metal complexes of block copolymers of PEO can have improved properties than that of complexes of PEO only.

Natural rubber (NR), an elastomer with good mechanical properties is an appropriate choice as a monomeric unit to improve stability of PEO *via* copolymerization. It is already reported the synthesis of NR/PEO block copolymers from our lab and find excellent mechanical and swelling properties [26]. Inspired from these knowledge we synthesized NR/PEO block

copolymer metal ion complexes *via* adsorption from aqueous medium. Block copolymer-metal ion complexes were subjected to different analytical techniques to understand the structure and properties of the metal complexes formed.

EXPERIMENTAL

Natural rubber (NR) of ISNR 5 grade was purchased from Rubber Research Institute of India, Kottayam, India. Polyethylene oxides (PEO) of molecular weight 6000, cobalt nitrate, nickel nitrate, copper sulphate and zinc sulphate were purchased from Merck India.

Preparation of NR/PEO block copolymer: The preparation of block copolymer was performed as per reported procedure [17].

Preparation of transition metal complexes of NR/PEO block copolymer: NR/PEO block copolymer (BC) sheet was cut into circular shaped disc having 2 cm diameter and leached in deionized water for 48 h to remove any unreacted material. The discs were then dried in a vacuum oven (60 ºC) for removing the water content. Dried samples after proper desiccation were used for the complexation studies. The polymer-metal complex was prepared by dipping the dried sample in the respective metal ion solution (40 mL of 20 mmol/L solution in deionized water) for 24 h to reach equilibrium. After allowing for the complexation, samples were taken out and washed with deionized water and kept at 60 ºC in vacuum oven. After proper desiccation the samples were used for analysis. Metal ion solution left after equilibrium period was analyzed using atomic absorption spectroscopy (AAS).

Characterization: FT-IR spectroscopy was recorded using Shimadzu IR Prestige-21 spectrometer. The absorption spectrum was recorded from 4000-650 cm^{-1} in ATR mode. ATR-FTIR spectrum was obtained using 20 scans at 4 cm^{-1} resolution and the spectrum of Zn-Se crystal in air serve as the background. XRD analysis were performed in Rigaku MiniFlex 600 powder X-ray diffractometer using Cu K_α radiation with step size 0.2, scan speed 3º/min and 40 kV/50mA.

Scanning electron microscopy: Prior to analysis, the sample was coated with gold and the imaging was performed on JSM - 640 Scanning Electron Microscope, JEOL.

Transmission electron microscopy: Transmission electron microscopy (TEM) was performed on a JEOL JEM-2010 high-resolution transmission electron microscope at an acceleration voltage of 120 kV. The samples were trimmed using a microtome machine. The specimen sections (*ca*. 70 nm in thickness) were placed on a 200 mesh copper grids for observation. Energy dispersive X-ray (EDX) spectroscopy is also done along with TEM.

RESULTS AND DISCUSSION

The metal ion chelating property of NR/PEO block copolymer is analyzed by calculating the percentage of metal ion complexed using the following equation:

$$\text{Metal ion complexed (\%)} = \frac{C_o - C_e}{C_o} \times 100$$

where C_o and C_e are the initial and equilibrium concentration of metal ions (mmol/L), respectively. NR/PEO block copolymer chelating exchanger can bind about 96 % of manganese ions and 63 % of iron metal ions from their respective metal ion solutions of 20 mmol/L concentration under pH~6, at room temperature for a time limit of 24 h. This revealed the high chelating ability of the prepared polymer chelating exchanger. This can swell in water and behave as hydrogel and as a result it is an excellent chelating exchanger for the complexation of metal ions.

FT-IR analysis: Herein, the FT-IR spectroscopy was used to confirm the formation of block copolymer, its interaction with the metal ions and the conformation of polyethylene oxide part of the block copolymer as well as the metal complexes.

The NR/PEO block copolymer was formed by the urethane linkage between rubber part and the polyethylene oxide part. The urethane linkage formation was identified by the FT-IR spectroscopy. The FT-IR spectrum of NR/PEO block copolymer (Fig. 1) shows a broad peak in the region 3600-3100 cm^{-1} corresponds to the N-H bond stretching and a peak corresponds to the C=O stretching at 1724 cm^{-1}, which indicates the formation of urethane linkage and is an evidence for the better copolymerization between the HTNR and PEO. A weak band at 1641 cm^{-1} may due to N-H bending . The next steps in FT-IR spectrum

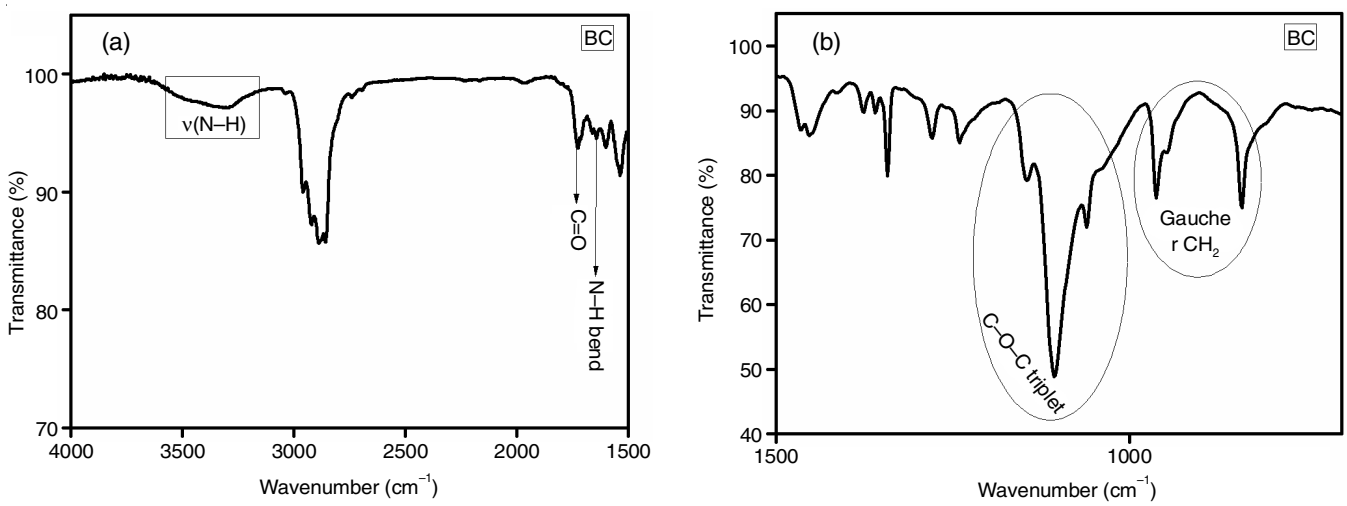

Fig. 1. FT-IR spectrum of NR/PEO block copolymer (a) formation of urethane linkage, (b) C-O-C triplet and CH_2 rocking

analysis were to identify the peaks corresponds to the NR part and of PEO and assign the conformation of PEO chains in the block copolymer which is the most important one.

The NR part comprises C-H and C=C vibrations and PEO has C-H and C-O-C vibrations. The saturated aliphatic C-H stretching vibrations of NR were observed at 2958 and 2920 cm^{-1}. The synthesized block copolymer shows peak representing the C=C stretching of natural rubber was observed at 1600 cm^{-1} (m) and 1658 cm^{-1} (w). The block copolymer shows a peak at 2887 and 2856 cm^{-1} in combination with the C-H vibrations of NR and is correspond to the C-H stretching of PEO. A very weak band at 1964 cm^{-1} is due to the overtone of PEO. The peaks in the range 1470-1230 cm^{-1} are assigned to the CH_2 scissoring, wagging and twisting modes which are indicated in Table-1. One of most important peaks of interest is the triplet peak of etheric C-O-C stretching. The semicrystalline nature of PEO was confirmed by the presence of C-O-C triplet peak. For pure PEO, the C-O-C triplet occur at 1147, 1103 and 1060 cm^{-1} with maximum intense peak at 1103 cm^{-1}. The prepared block copolymer shows the slightly shifted C-O-C stretching triplet peak at 1146, 1107 and 1060 cm^{-1}, which confirms the presence of semicrystalline phase of PEO in NR/PEO block copolymer [27,28].

TABLE-1
IR PEAK ASSIGNMENT OF BC

Peak (cm^{-1})	Assignment
3600-3100	N-H stretching of Urethane linkage
2958	C-H stretching of NR
2920	-CH_2 asymmetric stretching of NR
2887	CH_2 stretching of PEO
2856	CH_2 stretching of PEO
1964	Overtone of PEO
1724	C=O stretching of Urethane linkage
1658	-C=C- stretching
1641	N-H bending
1600	-C=C- stretching
1535	Aromatic C=C stretching
1465	CH_2 scissoring
1452	CH_2 scissoring
1375	CH_2 scissoring
1359	Symmetric CH_2 wagging + C-C stretching of PEO
1342	Asymmetric CH_2 wagging of PEO
1278	Asymmetric CH_2 twisting of PEO
1240	Asymmetric CH_2 twisting of PEO
1145	C-O-C triplet of PEO
1107	C-O-C triplet of PEO
1060	C-O-C triplet of PEO
962	Asymmetric CH_2 rocking of PEO } Gauche conformation
947	Symmetric CH_2 rocking of PEO } Gauche conformation
840	Asymmetric CH_2 rocking of PEO } Gauche conformation

According to the infrared spectral studies done by Davison [29] the CH_2 rocking modes of PEO in the 1000-700 cm^{-1} region were highly sensitive to the configuration. He assigned the two strong absorption peaks found in crystalline PEO at 844 and 947 cm^{-1}, while the peak at 960 cm^{-1} were for the *gauche* configuration of O-$(CH_2)_2$-O group. For a *trans* configuration of O-$(CH_2)_2$-O group the CH_2 rocking peaks will be observed at 773 and 992 cm^{-1}. Moreover, the dichroism for two C-O-C vibrations were perpendicular and propose a helical configuration of the methylene and C-O-C group of PEO. Later studies by number of authors [30-38] revealed that the PEO form a 7_2 helix with a 19.3 Å fibre axis and has a TTG conformation; *i.e*. *trans* (CC–OC), *trans* (CO–CC) and *gauche* (OC–OC). The gauche conformation of PEO part was confirmed by the FT-IR spectrum of the NR/PEO block copolymer which shows two absorptions at 840 cm^{-1} and 962-947 cm^{-1}. These findings suggested the presence of a TTG helical conformation in which the O-$(CH_2)_2$-O group in *gauche* configuration, *i.e.*, a tunnel is formed by seven monomeric units (CH_2CH_2O) in two turns of the helix. So we can assumed that the seven oxygens form the inner lining of the tunnel cavity and the CH_2 groups arranged in such a way that they face outward the tunnel with an approximate tunnel size 2.6-3.0 Å in diameter.

From the FT-IR studies, we can confirmed the block copolymerization *via* urethane linkage which binds the NR block and PEO block. We can also assume a semicrystalline nature of block copolymer and the 7_2 helical conformations. There are seven CH_2CH_2O chemical units and turns twice in a fibre identity period of 19.3 Å.

When the metal ions were binded to NR/PEO block copolymer, the binding takes place through the etheric oxygen atoms of PEO. The major changes were expected at C-O-C triplet and small variation in the CH_2 vibrations. The change in width of the etheric oxygen peaks and the CH_2 deformation peaks (broadening or shortening) and shift in frequencies account for the metal ion complexation. The FT-IR spectrum of block copolymer and its metal ion complexes are shown in Fig. 2. It is clear from the FT-IR spectrum of all the metal complexes retained all the peaks shown by the block copolymer. Upon alkali metal ions complexation, slight broadening of C-O-C triplet takes with increased intensity. The broadening of C-O-C triplet may be due to the metal-etheric oxygen interaction during the dative bond formation between metal ion and polymer and may also due to the overlapping of unbound C-O-C with that of bound C-O-C. All the metal complexes showed a change in peak width of C-O-C triplet and CH_2 deformation which indicate the interaction of etheric oxygen with the alkali metal cations. The absence of new peaks corresponding to *trans* O-$(CH_2)_2$-O group at 1000-700 cm^{-1} indicated the conformation of PEO chain of block copolymer of PEO part in block copolymer was unaltered by the metal ions. So the metal complex also has the TTG helical conformation in which the helix was formed in such a way that the methylene groups are oriented outward while the etheric oxygens inward to form a cavity. The PEO thus form a tunnel like arrangement in which the cavity was lined by the etheric oxygen. The metal ions entered into these cavities and coordinate to the etheric oxygen through dative bond formation in which the lone pair of oxygen was donated to the metal cation.

XRD analysis: X-ray diffraction spectroscopic analysis was performed in order to find out the structure and crystallization behaviour of block copolymer and its metal ion complexes. Here, the PEO acts as the metal ion binding ligand. As a result the major focus was on the changes of the crystalline peaks of PEO on block copolymerization as well as upon metal ion complexation. Here XRD studies were performed for pure PEO, block copolymer and block copolymer-metal complexes. In case of pure PEO, the crystalline peaks consisted of halo regions are

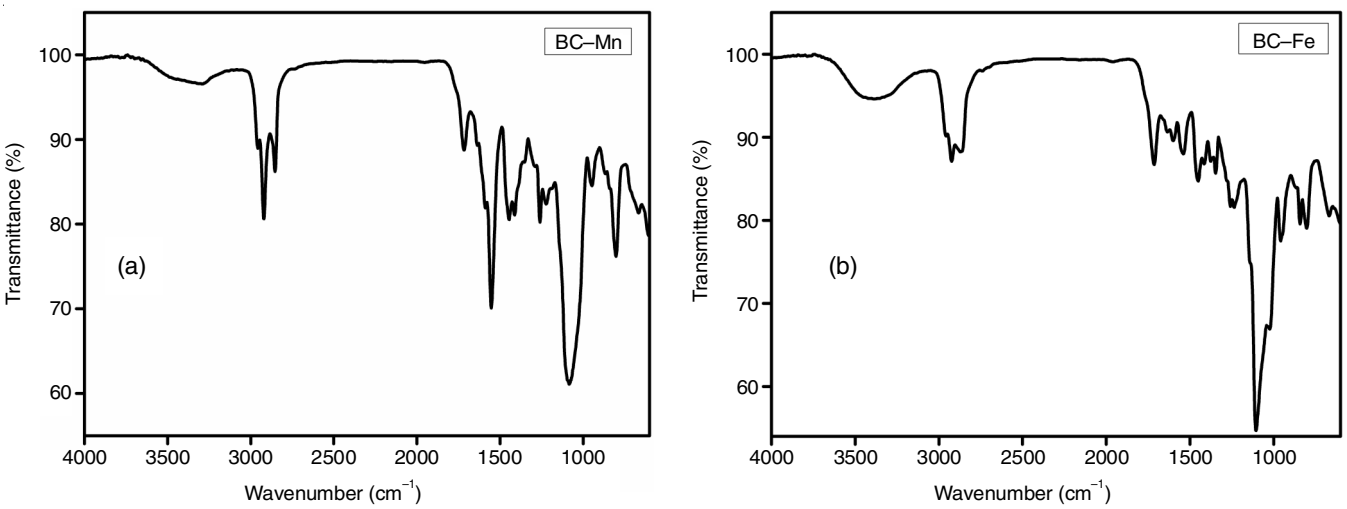

Fig. 2. FT-IR spectrum of BC–Metal complexes

appeared between 2θ values 15º to 30º and prominent peaks are appear at 2θ = 19.2º, 23.3º and weak peaks observed at 2θ = 13.5º, 14.6º, 21º, 22º, 26.1º, 26.8º, 27.8º, 30.8º, 36.2º and 39.6º indicating a monoclinic crystalline structure. The XRD spectra of PEO, block copolymer and block copolymer-metal complexes are shown in Fig. 3. The natural rubber showed a broad peak at 30º due its long range stereo regular amorphous state and a weak peak at around 19º due to self-crystallization property. The block copolymer shows crystalline peaks and halo region simultaneously which indicated the semicrystalline nature of prepared block copolymer. It shows two prominent crystalline peaks at 2θ values 19.6º and 23.6º with highest intensity and other low intensity peak at 26.7º, 36.4º and 40.2º, which indicate the presence of crystalline phase of PEO in the polymer. The broad bump in 2θ values 15-30 may be due to the combined effect of amorphous nature of rubber and that due to the halo space in case of PEO. This indicates that the prepared polymer contains the crystalline and amorphous phases and is semi-crystalline in nature.

Upon metal ion complexation, the etheric oxygen coordinate with metal cation and may lead to the deformations or destruction of PEO crystal structure. Block copolymer-Mn(II) complex shows all the peaks of block copolymer shifted towards low 2θ value with increased peak height and bump area. The intensity and position of peaks of block copolymer will change upon metal ion complexation in order to accommodate the metal ion into the lattice. Depending upon the metal ion size, the PEO lattice either expands or contracts and peaks will respectively shifted to lower or higher angles (*i.e.* 2θ values). The increase in intensity of peaks compared to that of block copolymer may due to the electron density difference of complexed material. The iron complex showed an increased bump height with peaks with reduced intensity. It retained all the major peaks of block copolymer and at the same time the peaks corresponding to the metal salt was absent. The absence of peaks corresponding to the metal salt indicates the better complexation of metal ions to etheric oxygen in the block copolymer. The average crystallite size of the samples was calculated using Scherrer's equation and found that crystallite size vary upon metal ion complexation. The block copolymer showed an average crystallite size of 12.4 nm where as it increased to 16.9 and 19.4 nm upon manganese and iron complexation, respectively which indicates an increased amorphousity in the sample.

EDX analysis: Qualitative elemental compositional analysis of block copolymer and its Mn(II) & Fe(II) complexes was

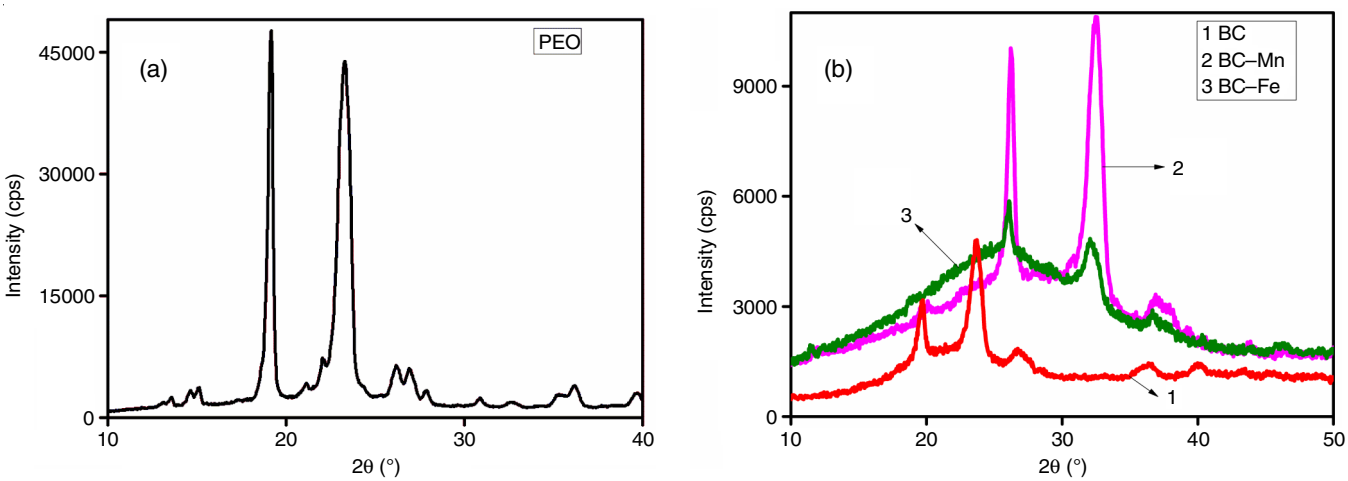

Fig. 3. XRD spectrum of pure (a) PEO and (b) BC and BC–M complexes

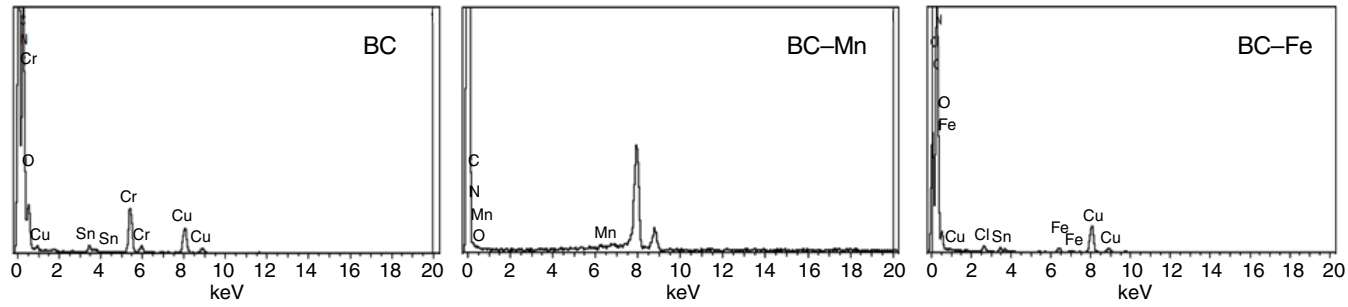

Fig. 4. EDX spectrum of BC and its complexes

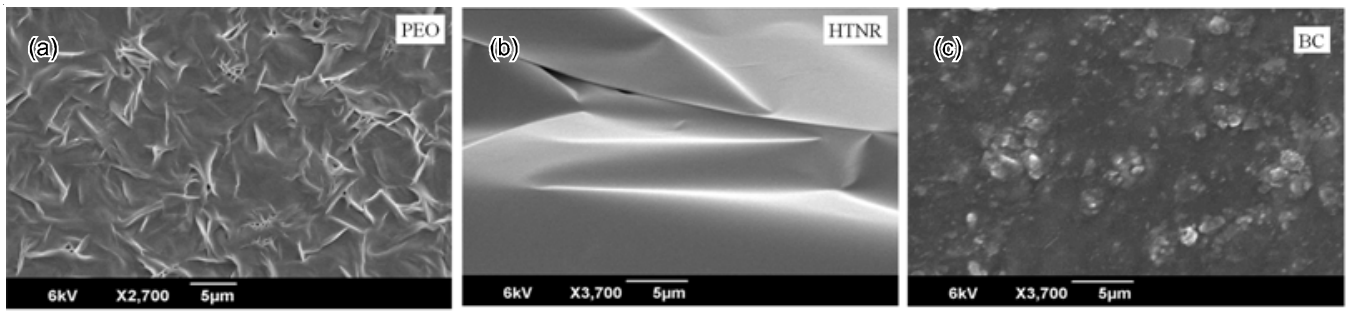

Fig. 5. Scanning electron micrographs of (a) PEO, (b) HTNR and (c) BC

done *via* EDX analysis. In EDX spectrum, the peaks represent the possible transitions in electron shells of elements. Positions of peaks are unique and are characteristic of each element. The EDX spectrum of block copolymer, block copolymer-Mn(II) complex and block copolymer-Fe(III) are shown in Fig. 4.The EDX spectrum of block copolymer shows the presence of C, N and O at 0.27, 0.39 and 0.5 keV, respectively which correspond to their $K\alpha_1$ X-ray emission energy. Other two peaks observed at ~ 8.0 and 8.9 keV represent the Cu $K\alpha_2$ and Cu $K\alpha_1$ lines, respectively arising from the copper grid. The peak corresponds to $K\alpha_1$ X- ray emission of N at 0.39 keV supports the urethane linkage formation. The EDX spectrum of block copolymer-Mn(II) complex shows the peaks arise from block copolymer and grid along with peaks of manganese. Block copolymer-Mn(II) complex shows peaks at 6.49 and 0.5 keV indicates the presence of manganese which corresponds to $K\beta_{1,3}$ and L1 X-ray emission energies, respectively. The complexation of iron and block copolymer is confirmed by the EDX spectrum which shows peaks of Fe at ~ 0.7, 6.4 and 7.0 keV due to combined effect of $L\alpha_{1,2}$ and $L\beta_1$, $K\alpha_{1,2}$ and $K\beta_{1,3}$ X-ray emissions respectively. The $K\alpha_{1,2}$ emission peak of chlorine may arise from the iron chloride salt used. All the major peaks of block copolymer also observed in the spectrum.

SEM analysis: Scanning electron microscopy gives the surface topography and composition of the sample by scanning the surface with focused beam of electrons. The surface topology of HTNR, PEO and block copolymer are shown in Fig. 5. Pure PEO (Fig. 5a) shows a rough surface morphology with many beautiful rumples while the amorphous HTNR shows a smooth surface morphology (Fig. 5b). When block copolymerized morphology changed from that of monomers and form a phase separated rough surface morphology is obtained for block copolymer which is shown in Fig. 5c. But the surface roughness is less than pure PEO and surface is uniformly distributed by small circular shaped domains.

When metal ion complexation occured, the surface morphology of block copolymer changes dramatically as shown in Fig. 6. The manganese complex showed a rough morphology with spherical patterns arranged in a particular region. The iron complex shows a rough surface with no spherical regions but showed many folding and smoother than that of block copolymer due to decrease in crystallinity.

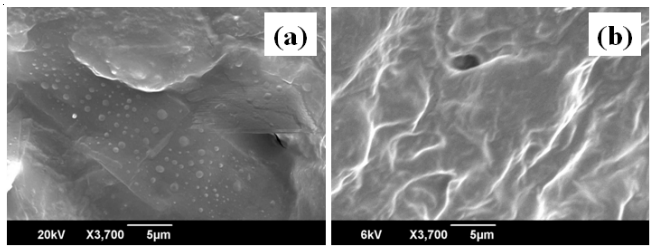

Fig. 6. SEM images of (a) BC–Mn and (b) BC–Fe

TEM analysis: To further understand the detailed morphology and the mechanism of complexation transmission electron microscopic analysis was done. The TEM images of block copolymer and block copolymer-metal ion complexes are shown in Fig. 7. It shows phase separated morphology in which the dark spherical domain is surrounded by light regions and can assume a micelle formation. The preferential adsorption leads to the formation of dark and light regions in the images. The region where high absorption occurs appears dark while lower absorption region appear light. Due to the crystallinity and high cohesive energy density the absorption is higher (*i.e.* lower number of transmitted electrons) for PEO and appear as dark. Natural rubber absorbs less due to low cohesive energy and appears as light phase. When metal ions are coordinated with block copolymer the major changes taking place in the micelle formation. Higher loading of manganese metal ions on block co-polymer was clearly seen from the TEM results (Fig. 7b).

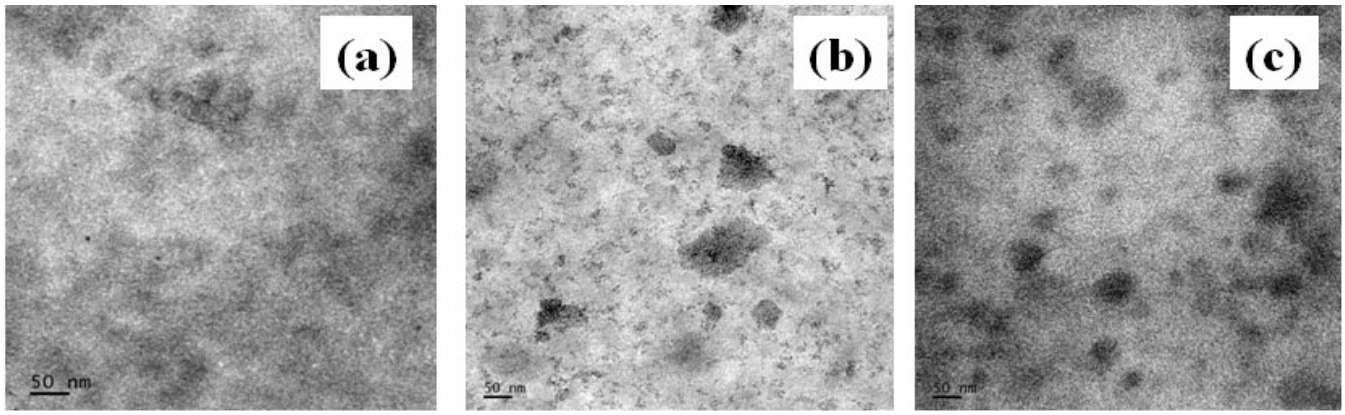

Fig. 7. TEM images of (a) BC, (b) BC–Mn and (c) BC–Fe

Small micelles and aggregation of micelles are observed throughout the surface almost in a uniform manner. Due to the perfect size matching of manganese metal ion and the PEO cavity bare minimum number of monomeric units wrap around a single metal ion and may lead to the formation of smaller micelles. The iron leaded micelles do not form a perfect circular shape but frequently seen at the surface.

Conclusion

NR/PEO-metal ion chelates are prepared *via* solution batch adsorption method. The adsorption studies revealed that 96 % and 63 % of manganese and iron ions are complexed with NR/PEO block copolymer chelating exchanger, respectively. FT-IR analysis of prepared polymer chelating exchanger and its metal ion chelates reveals 7_2 helical conformation of PEO. The decrease in intensity and broadening of C-O-C triplet indicates that the metal ions complexes are formed *via* coordination through etheric oxygen atoms. It also indicates the semicrystalline nature of PEO in the samples studied. So each metal ion can enter into the PEO cavity and can bind with 7 or < 7 etheric oxygens depending on their respective stability requirements. The semicrystalline nature, etheric oxygen-metal ion coordination and increased amorphosity are also confirmed by XRD analysis. The presence of metal ions in the polymer chelate is qualitatively identified using EDX analysis. A rough surface morphology and micellar formation are revealed by SEM and TEM analyses. All the above mentioned studies revealed a good chelating effect of NR/PEO block copolymer towards the metal ion [Mn(II) and Fe(III)].

CONFLICT OF INTEREST

The authors declare that there is no conflict of interests regarding the publication of this article.

REFERENCES

1. B.L. Rivas, H.A. Maturana, M.J. Molina, M.R.G. Anton and I.F. Piérola, *J. Appl. Polym. Sci.*, **67**, 1109 (1998); https://doi.org/10.1002/(SICI)1097-4628(19980207)67:6<1109::AID-APP19>3.0.CO;2-V.
2. M.J. Tiera, V.A. De Oliveira, H.D. Burrows, M. Graça Miguel and M.G. Neumann, *Colloid Polym. Sci.*, **276**, 206 (1998); https://doi.org/10.1007/s003960050230.
3. T. Siyam, A.H. Ashour and H.A. Youssef, *Polym. Int.*, **48**, 799 (1999); https://doi.org/10.1002/(SICI)1097-0126(199909)48:9<799::AID-PI157>3.0.CO;2-J.
4. S. Varghese, A.K. Lele, D. Srinivas and R.A. Mashelkar, *J. Phys. Chem. B*, **105**, 5368 (2001); https://doi.org/10.1021/jp002310+.
5. E.A. Bekturov and G.K. Mamutbekov, *Macromol. Chem. Phys.*, **198**, 81 (1997); https://doi.org/10.1002/macp.1997.021980107.
6. L. Jose and V.N.R. Pillai, *Macromol. Chem. Phys.*, **197**, 2089 (1996); https://doi.org/10.1002/macp.1996.021970702.
7. T. Suzuki, Y. Murakami and Y. Takegami, *Polym. J.*, **14**, 431 (1982); https://doi.org/10.1295/polymj.14.431.
8. M.A.R. Meier, D. Wouters, C. Ott, P. Guillet, C.-A. Fustin, J.-F. Gohy and U.S. Schubert, *Macromolecules*, **39**, 1569 (2006); https://doi.org/10.1021/ma052045w.
9. S.J. Buwalda, P.J. Dijkstra and J. Feijen, *J. Polym. Sci. A Polym. Chem.*, **50**, 1783 (2012); https://doi.org/10.1002/pola.25945.
10. N. Martinez-Castro, Z. Zhou and G. Liu, *Polymer*, **51**, 2629 (2010); https://doi.org/10.1016/j.polymer.2010.04.036.
11. F. Quina, L. Sepulveda, R. Sartori, E.B. Abuin, C.G. Pino and E.A. Lissi, *Macromolecules*, **19**, 990 (1986); https://doi.org/10.1021/ma00158a010.
12. K.-J. Liu, *Macromolecules*, **1**, 308 (1968); https://doi.org/10.1021/ma60004a005.
13. K. Liu and J.E. Anderson, *Macromolecules*, **2**, 235 (1969); https://doi.org/10.1021/ma60009a004.
14. K. Ono, H. Konami and K. Murakami, *J. Phys. Chem.*, **83**, 2665 (1979); https://doi.org/10.1021/j100483a024.
15. P.A. Banka, J.C. Selser, B. Wang, D.K. Shenoy and R. Martin, *Macromolecules*, **29**, 3956 (1996); https://doi.org/10.1021/ma9518159.
16. H. Tadokoro, Y. Chatani, T. Yoshihara, S. Tahara and S. Murahashi, *Chem. Macromol. Chem. Phys.*, **73**, 109 (1964); https://doi.org/10.1002/macp.1964.020730109.
17. L.H. Sim, S.N. Gan, C.H. Chan and R. Yahya, *Spectrochim. Acta A Mol. Biomol. Spectrosc.*, **76**, 287 (2010); https://doi.org/10.1016/j.saa.2009.09.031.
18. N. Vasanthan, I.D. Shin and A.E. Tonelli, *Macromolecules*, **29**, 263 (1996); https://doi.org/10.1021/ma950829b.
19. B.L. Papke, M.A. Ratner and D.F. Shriver, *J. Phys. Chem. Solids*, **42**, 493 (1981); https://doi.org/10.1016/0022-3697(81)90030-5.
20. T. Himba, *Solid State Ion.*, **9-10**, 1101 (1983); https://doi.org/10.1016/0167-2738(83)90137-6.
21. L. Paternostre, P. Damman and M. Dosire, *J. Polym. Sci. B: Polym. Phys.*, **37**, 1197 (1999); https://doi.org/10.1002/(SICI)1099-0488(19990615)37:12<1197::AID-POLB1>3.0.CO;2-C.
22. R. Caminiti, M. Carbone, S. Panero and C. Sadun, *J. Phys. Chem. B*, **103**, 10348 (1999); https://doi.org/10.1021/jp991320b.
23. D. Cohn and A.H. Salomon, *Polymer*, **46**, 2068 (2005); https://doi.org/10.1016/j.polymer.2005.01.012.
24. C.V. Bonduelle, S. Karamdoust and E.R. Gillies, *Macromolecules*, **44**, 6405 (2011); https://doi.org/10.1021/ma2009996.

25. J. Wu, Y.S. Thio and F.S. Bates, *J. Polym. Sci. B: Polym. Phys.*, **43**, 1950 (2005); https://doi.org/10.1002/polb.20488.
26. T. Ravindran, M.R.G. Nayar and D.J. Francis, *J. Appl. Polym. Sci.*, **42**, 325 (1991); https://doi.org/10.1002/app.1991.070420204.
27. S.A.M. Noor, A. Ahmad, I.A. Talib and M.Y.A. Rahman, *Ionics*, **16**, 161 (2010); https://doi.org/10.1007/s11581-009-0385-6.
28. A.M. Rocco, C.P. da Fonseca and R.P. Pereira, *Polymer*, **43**, 3601 (2002); https://doi.org/10.1016/S0032-3861(02)00173-8.
29. W.H.T. Davison, *J. Chem. Soc.*, 3270 (1955); https://doi.org/10.1039/jr9550003270.
30. B.L. Papke, M.A. Ratner and D.F. Shriver, *J. Electrochem. Soc.*, **129**, 1434 (1982); https://doi.org/10.1149/1.2124179.
31. R. Iwamoto, Y. Saito, H. Ishihara and H. Tadokoro, *J. Polym. Sci. A*, **6**, 1509 (1968); https://doi.org/10.1002/pol.1968.160060808.
32. H. Matsuura and K. Fukuhara, *J. Polym. Sci. B: Polym. Phys.*, **24**, 1383 (1986); https://doi.org/10.1002/polb.1986.090240702.
33. S. Bollas, K. Chrissopoulou, K.S. Andrikopoulos, G.A. Voyiatzis and S.H. Anastasiadis, *Polymers*, **9**, 73 (2017); https://doi.org/10.3390/polym9020073.
34. G.D. Smith, D. Bedrov and O. Borodin, *J. Am. Chem. Soc.*, **122**, 9548 (2000); https://doi.org/10.1021/ja001053j.
35. H. Tadokoro, Y. Chatani, T. Yoshihara, S. Tahara and S. Murahashi, *Makromol. Chem.*, **73**, 109 (1964); https://doi.org/10.1002/macp.1964.020730109.
36. H. Tadokoro, M. Kobayashi, Y. Kawaguchi, A. Kobayashi and S. Murahashi, *J. Chem. Phys.*, **38**, 703 (1963); https://doi.org/10.1063/1.1733727.
37. R. Yamadera, H. Tadokoro and S. Murahashi, *J. Chem. Phys.*, **41**, 1233 (1964); https://doi.org/10.1063/1.1726055.
38. T. Yoshihara, H. Tadokoro and S. Murahashi, *J. Chem. Phys.*, **41**, 2902 (1964); https://doi.org/10.1063/1.1726373.